

1 Induction of mitochondrial heat shock proteins and mitochondrial biogenesis in  
2 endothelial cells upon acute methylglyoxal stress: Evidence for hormetic  
3 autofeedback

4

5 Acute methylglyoxal stress induces hormetic autofeedback in endothelial cells

6

7 Ruben Bulkescher <sup>1</sup>, Thomas Fleming <sup>1,2</sup>, Claus Rodemer <sup>1</sup>, Rebekka Medert <sup>3</sup>, Marc Freichel <sup>3</sup>,

8 Matthias Mayer <sup>4,5</sup>, Julia Szendroedi <sup>1,2,6</sup>, Stephan Herzig <sup>6,7,8</sup>, Johanna Zemva <sup>1,\*</sup>

9

10 <sup>1</sup> Department of Internal Medicine I and Clinical Chemistry, University Hospital Heidelberg, Heidelberg,  
11 Germany

12  
13 <sup>2</sup> German Center for Diabetes Research (DZD), 85764 Neuherberg, Germany

14  
15 <sup>3</sup> Institute of Pharmacology, University of Heidelberg, Heidelberg, Germany

16  
17 <sup>4</sup> Center for Molecular Biology of Heidelberg University (ZMBH), Heidelberg, Germany

18  
19 <sup>5</sup> DKFZ-ZMBH Alliance, Heidelberg, Germany

20  
21 <sup>6</sup> Joint Heidelberg-IDC Translational Diabetes Program, Internal Medicine I, Heidelberg University Hospital,  
22 Heidelberg, Germany

23  
24 <sup>7</sup> Institute for Diabetes and Cancer (IDC), Helmholtz Center Munich, Neuherberg, Germany

25  
26 <sup>8</sup> Chair Molecular Metabolic Control, Technical University Munich, Munich, Germany

27  
28 \* Corresponding author.

29 E-Mail: [johanna.zemva@med.uni-heidelberg.de](mailto:johanna.zemva@med.uni-heidelberg.de) (JZ)

30 **Abstract**

31 Increased metabolic flux produces potentially harmful side-products, such as reactive  
32 dicarbonyl and oxygen species. The reactive dicarbonyl methylglyoxal (MG) can impair  
33 oxidative capacity, which is downregulated in type 2 diabetes. Heat shock proteins (HSPs) of  
34 subfamily A (Hsp70s) promote ATP-dependent processing of damaged proteins during MG  
35 exposure which also involve mitochondrial proteins. Since the protection of mitochondrial  
36 proteins could promote higher production of reactive metabolites due to increased  
37 substrate flux, tight regulation of HspA-mediated protein handling is important. We  
38 hypothesized that stress-inducible HspAs (HspA1A/HspA1B) are pivotal for maintaining  
39 mitochondrial biogenesis during acute MG-stress. To analyze the role of stress-inducible  
40 HspA1A/HspA1B for maintenance of mitochondrial homeostasis during acute MG exposure,  
41 we knocked out HSPA1A/HSPA1B in mouse endothelial cells. HSPA1A/HSPA1B KO cells  
42 showed upregulation of the mitochondrial chaperones HspA9 (mitochondrial  
43 Hsp70/mortalin) and HspD1 (Hsp60) as well as induction of mitochondrial biogenesis upon  
44 MG exposure. Increased mitochondrial biogenesis was reflected by elevated mitochondrial  
45 branching, total count and area as well as by upregulation of mitochondrial proteins and  
46 corresponding transcription factors. Our findings suggest that mitochondrial HspA9 and  
47 HspD1 promote mitochondrial biogenesis during acute MG stress, which is counterregulated  
48 by HspA1A/HspA1B to prevent mitochondrial overstimulation and to maintain balanced  
49 oxidative capacity under metabolic stress conditions. These data support an important role  
50 of HSPs in MG-induced hormesis.

51 **1. Introduction**

52 During increased metabolic flux, reactive side-products are inevitably produced, such as  
53 reactive dicarbonyls from glycolysis or reactive oxygen species (ROS) from oxidative  
54 phosphorylation. The concept of hormesis, meaning that low doses of a substance are  
55 beneficial whereas high doses are toxic, is well defined for a broad spectrum of metabolites  
56 (1). Next to physical and chemical agents, intrinsic metabolites were shown to induce  
57 hormetic reactions in model organisms but also in humans. Accordingly, beneficial effects  
58 achieved by physical training were diminished by simultaneous supplementation of  
59 antioxidants, possibly via scavenging of ROS thereby inhibiting ROS-induced mitohormesis  
60 (2). Moreover, mitochondrial adaptation to increased substrate flux and ROS-production was  
61 shown to counteract the development of steatosis and steatohepatitis in non-alcoholic fatty  
62 liver disease (NAFLD) (3). The reactive dicarbonyl methylglyoxal (MG) was described to  
63 induce a hormetic reaction by increasing cell survival to different stressors in yeast cells (4)  
64 and healthy aging in *C. elegans* (5). However, it stays unclear, if MG-induced hormesis is also  
65 relevant in the mammalian system and if it also involves mitochondrial capacity.

66

67 Under physiological conditions, MG is predominantly formed as a spontaneous by-product  
68 from the intermediates glyceraldehyde 3-phosphate and dihydroxyacetone phosphate  
69 (triosephosphates) during glycolysis (6, 7). MG can react with and thereby modify proteins,  
70 lipids, and DNA, resulting in the formation of advanced glycation endproducts (AGEs) (8).  
71 Regarding protein modifications, the most abundant adduct is the modification of arginine  
72 residues, also called hydroimidazolone or MG-H1 (7, 8). Posttranslational modifications of  
73 proteins lead to conformational changes, impaired function, and increased risk of  
74 aggregation. MG and AGEs have been shown to be involved in the development and

75 progression of diabetic complications, such as diabetic nephropathy (9-12) or cardiovascular  
76 disease (13, 14). AGEs also contribute to reduced oxidative capacity, which is a hallmark of  
77 diabetic complications, and has been shown to relate to insulin resistance and NAFLD (15).  
78 Also, MG has been linked to mitochondrial dysfunction, which is supported by the  
79 identification of MG-modifications within the mitochondria (16-19). Micro- and  
80 macrovascular damage is one of the major drivers of diabetic complications and is  
81 characterized by endothelial disruption. However, the exact mechanisms linking increased  
82 AGE formation and mitochondrial dysfunction in endothelial cells is still to be unraveled.

83

84 Heat shock proteins (HSPs) are critical for diverse cellular housekeeping functions, including  
85 refolding misfolded or damaged proteins (20, 21). Modified proteins cannot be solely  
86 removed by molecular chaperones or HSPs but require further components of the protein  
87 quality control (PQC), like the proteasome or autophagy. However, HSPs can prevent the  
88 aggregation of modified proteins and play a central role in protecting cells from proteotoxic  
89 stress (22). The HspA/Hsp70 family comprises ATP-dependent chaperones with several  
90 members, sharing similar structure and function (23). The stress-inducible members HspA1A  
91 and HspA1B are predominantly expressed in the cytosol, highly homologous and can fully  
92 compensate each other reflecting mutual regulation of HSPs. The constitutively expressed  
93 cytosolic member HspA8 or Hsc70 is essential for housekeeping functions (24). HspA9, also  
94 called mtHsp70 or mortalin, is a compartment-specific member and exclusively expressed in  
95 the mitochondria. While mitochondrial HSPs can be upregulated upon the mitochondrial  
96 unfolded protein response (mtUPR) (25) or during mitochondrial biogenesis (26), complete  
97 knockout of HspA8 or HspA9 is lethal (27). In the absence of ATP, HspA family members  
98 strongly bind to misfolded proteins and are released upon ATP binding to the N-terminal

99 region. ATP-binding, hydrolysis (for example by members of the Dnaj/Hsp40 family) and  
100 removing of ADP is facilitated by co-chaperones or small heat shock proteins (28). This cycle  
101 of binding and release of the misfolded protein is repeated until complete refolding is  
102 achieved (29). Therefore, regulation of the cellular energy level and of mitochondrial  
103 biogenesis are critical for efficient functioning of the PQC. Furthermore, mitochondrial  
104 dynamics including fission and fusion are essential for mitochondrial PQC and homeostasis  
105 (30). Fusion contributes to mitochondrial elongation and maintains cellular oxidative  
106 capacity (31) whereas fission can induce a highly fragmented mitochondrial network  
107 resulting in decreased ATP production (32). Therefore, the cellular ATP-levels are highly  
108 dependent on the overall mitochondrial mass and interconnection. However, it is still  
109 unclear how the cell regulates or compensates increased ATP-demand upon rising  
110 proteotoxic stress.

111

112 In line with this, patients with type 2 diabetes show decreased levels of the key-regulator of  
113 mitochondrial biogenesis Ppargc1a (Peroxisome proliferator-activated receptor gamma  
114 coactivator 1-alpha) (33) and Ppargc1a responsive genes involved in oxidative  
115 phosphorylation (34).

116 The HspA family is found to be involved in many disease conditions, including type 1 and  
117 type 2 diabetes (T2D) (35, 36). Single nucleotide polymorphisms (SNPs) of HSPA1A/HSPA1B  
118 have been linked to the development of diabetic nephropathy in T2D (37-39). Furthermore,  
119 decreased expression of skeletal HspA1A/HspA1B has been shown to be associated with  
120 insulin resistance (40, 41). A negative correlation with age has been reported for  
121 HspA1A/HspA1B in T2D (42). Apart from HspA1A/HspA1B, the mitochondrial expressed  
122 HspD1 (Hsp60) and the small HspB1 (Hsp27) have also been linked to micro- and

123 macrovascular complications in T2D (43-45). So far, the role of HSPs in preventing  
124 accumulation of MG-modified proteins and preserving mitochondrial homeostasis under  
125 acute MG stress is still unknown.

126

127 To understand the role of HSPs for maintenance of mitochondrial homeostasis during rising  
128 proteotoxic stress, and the mutual regulation of different HSPs, we analyzed the effect of  
129 acute MG-exposure on mitochondrial biogenesis and HSPs in mouse cardiac endothelial cells  
130 (MCECs). We hypothesized that this would aggravate accumulation of MG-modified proteins  
131 and disrupt mitochondrial homeostasis upon acute MG-stress. Furthermore, we questioned  
132 if induction of MG-driven hormesis would be diminished in the absence of stress-inducible  
133 HSPA1A/HSPA1B, as the yeast homologue of HSPA1A/HSPA1B was shown to be a key  
134 mediator of the MG-induced defense response (4).

## 135 **2. Material and Methods**

### 136 *2.1 Cell culture*

137 An immortalized mouse cardiac endothelial cell (MCEC) line was obtained from Cellutions  
138 Biosystems (#CLU510). Cells were cultivated in DMEM (Gibco, #31885023) supplemented  
139 with 5% FCS (Sigma, #F4135), 1% penicillin (10,000 Units/ml) (Gibco), 1% streptomycin (10  
140 mg/ml) (Gibco), 1% amphotericin B (250 µg/ml) (Gibco) and 1 mM HEPES (Gibco) in a  
141 humidified atmosphere at 37 °C and 5% CO<sub>2</sub>. Cells were grown to full confluency and then  
142 passaged with 0.05% Trypsin (Gibco) in gelatin-coated (0.5% in PBS for 15 minutes) cell  
143 culture flasks. All cell lines were regularly tested for mycoplasma contamination.

144

### 145 *2.2 Generation of HSPA1A/HSPA1B knockout cell line*

146 1x10<sup>6</sup> cells were transfected (Neon Transfection System, Invitrogen) with two vectors from  
147 Sigma-Aldrich, targeting the two stress-inducible Hsp70 variants Hspa1a (Gene ID: 193740;  
148 targeting sequence of the gRNA: TGTGCTCAGACCTGTTCCG) and Hspa1b (Gene ID: 15511;  
149 targeting sequence of the gRNA: CGGTTCGAAGAGCTGTGCT). Both vectors contained one of  
150 the respective gRNA target sequences, the Cas9 endonuclease gene and a fluorescent  
151 reporter gene (GFP for Hspa1a and RFP for Hspa1b). Fluorescence activated cell sorting  
152 (FACS) was performed to detect and isolate GFP and RFP expressing cells. Clones were  
153 cultured and genome, mRNA and protein analysis were performed to confirm successful  
154 knockout of HSPA1a/HSPA1B. Cell clones AD4 and BE12 were confirmed as full double  
155 knockout clones of both genes on the genome, mRNA and protein level. The third clone BH9  
156 was confirmed as a full double knockout clone on the mRNA and protein level.

157

### 158 *2.3 Methylglyoxal treatment*

159 75,000 cells/cm<sup>2</sup> were seeded in a gelatin-coated (0.5% in PBS for 15 minutes) cell culture  
160 dish (T75-flask or 60mm petri dish or 96-well plate). The next day, cells were washed with  
161 PBS and replaced with medium containing 0.1% FCS (assay medium) for 1 hour. Then,  
162 methylglyoxal (Sigma-Aldrich) was added to the assay medium to a concentration of 500 µM  
163 and added to the cells. Only assay medium was added to the control. For RNA  
164 measurements (RT-qPCR and mRNA-Seq) the cells were harvested after 12 hrs, for protein  
165 measurements (Fluorescence microscopy and Western blotting) cells were fixed or  
166 harvested after 24 hrs.

167

#### 168 *2.4 Immunocytochemistry and Fluorescence microscopy*

169 For immunofluorescent staining, cells were fixed with 4% paraformaldehyde solution for 20  
170 min at RT and permeabilized with 0.1% Triton X-100 for 8 min. Then, blocking was  
171 performed with 3% BSA in PBS for 60 min. All primary antibodies were added in blocking  
172 buffer in dilutions of 1:50 – 1:300 and incubated overnight at 4 °C. All secondary antibodies  
173 were added in blocking buffer in a dilution of 1:1000 and incubated for 2 hrs at RT. Nuclear  
174 counterstaining was performed with Hoechst 33342 (#H3570, Molecular Probes) with a  
175 working solution of 1 µg/mL in PBS for 1 min 30 sec at RT. Between all steps, the cells were  
176 washed three times for 5 min with 1× PBS at RT. A list of all antibodies can be found in the  
177 supplementary material (Supplementary material Table S1).

178 For the acquisition of the images, the automated screening widefield microscope IX81 from  
179 Olympus was used, with the ScanR acquisition software. The images were taken with a 60X  
180 objective and the following filters: DAPI filter (absorption maximum: 358 nm; emission  
181 maximum: 461 nm; for detection of cell nuclei stained with Hoechst 33342); GFP filter  
182 (absorption maximum: 395 nm; emission maximum: 475 nm), Cy3 filter (absorption



183 maximum: 550 nm; emission maximum: 570 nm), and Cy5 filter (absorption maximum: 650  
184 nm; emission maximum: 670 nm). Image analysis was performed using the Java-based image  
185 processing program ImageJ (<http://imagej.nih.gov/ij/>) and KNIME software  
186 ([www.knime.org](http://www.knime.org)).

187

### 188 *2.5 RNA isolation and Reverse-transcription quantitative PCR (RT-qPCR)*

189 RNA isolation was performed with the RNeasy Mini Kit (Qiagen) according to the  
190 manufacturer's protocol. cDNA transcription was performed with the High-Capacity cDNA  
191 Reverse Transcription Kit (Applied Biosystems) according to the manufacturer's protocol. RT-  
192 qPCR was performed using PowerUp™ SYBR™ Green Master Mix (Applied Biosystems) on a  
193 StepOnePlus™ Real-Time PCR System (Applied Biosystems).

194 Signals of amplified products were verified using melting curve analysis and mRNA levels  
195 were normalized to Hypoxanthine-guanine phosphoribosyl transferase (Hprt, Gene ID:  
196 15452). The fold-changes in gene expression levels were calculated using the  $\Delta\Delta C_t$  method.  
197 Primer sequences used for analyzing mRNA can be found in the supplementary material  
198 (Supplementary material Table S1).

199

### 200 *2.6 MG-H1 clearance assay*

201 24 hrs after treatment (see 2.3), MG-containing assay medium was removed, the cells were  
202 washed with PBS three times and assay medium was added to the cells. The plates were  
203 fixed at 0, 24 and 48 hrs after MG removal and stained according to 2.4. The plates were  
204 measured on an Odyssey DLx Imaging system (LI-COR) and analyzed using Image Studio™  
205 Lite (<https://licor.com/bio/image-studio-lite/>).

206

## 207 *2.7 Mitochondrial network analysis (imageJ plugin)*

208 Mitochondrial network analysis was performed with a self-made imageJ plugin/macro. For  
209 this, images were acquired as z-stacks of a total of 30 layers with a step size of 200 nm,  
210 followed by deconvolution using the Huygens professional software  
211 (<https://svi.nl/HomePage>). Settings that can be modified were image processing  
212 (background subtraction), thresholding, size and shape discrimination, binary image  
213 processing and mitochondria network branching analysis. The images were first converted to  
214 a binary mask and then skeletonized. The skeletonized images were then analyzed regarding  
215 number, size, and signal intensity of the particles. For the mitochondrial signal, locations  
216 with three or more neighboring pixels were counted as branches/junctions. A more detailed  
217 depiction of the complete workflow can be found in the supplementary material  
218 (Supplementary Text S2).

219

## 220 *2.8 Western blotting*

221 20 µg protein of the cell lysates (see 2.8) were mixed with 4x Laemmli buffer and heated to  
222 95°C for 5 min. The separation was done in a Mini-PROTEAN® TGX (Bio-Rad) precasted gel  
223 (4–20% acrylamide) at 150V for 75 min. Proteins were transferred on a nitrocellulose  
224 membrane in a Trans-Blot® Turbo™ Transfer System (Bio-Rad) and blocked with 5% non-fat  
225 dry milk in PBS or protein-free blocking buffer (Pierce) containing 5% goat serum for 1 hour at  
226 RT. When necessary, endogenous biotin sites were blocked with the avidin/biotin blocking  
227 kit from Linaris following the manufacturer's protocol. Membranes were incubated with the  
228 primary antibody in blocking buffer at 4 °C overnight, and incubated with the secondary  
229 antibody in blocking buffer for 1 hour at RT. Between all steps, the membranes were washed  
230 three times for 10 min with 1× TBS-Tween20 (0.1% (v/v)) at RT. The bands were detected on

231 a ChemiDoc imaging system (Bio-Rad) with ECL detection reagent (GE Healthcare) or on an  
232 Odyssey DLx Imaging system (LI-COR) and analyzed using imageJ (<http://imagej.nih.gov/ij/>)  
233 or Image Studio™ Lite (<https://licor.com/bio/image-studio-lite/>).

234

### 235 *2.9 Statistical analysis*

236 Experimental results are expressed as mean  $\pm$  standard deviation or, where stated, as mean  
237  $\pm$  standard error of the mean. Depending on the experimental setup, statistical significance  
238 was analyzed using ordinary one-way or two-way ANOVA. The analysis was performed with  
239 GraphPad Prism software (<https://www.graphpad.com/>) and p-values  $< 0.05$  were  
240 considered statistically significant.

241 **3. Results**

242 *3.1 MG-H1 accumulation is higher in HSPA1A/HSPA1B KO compared to WT cells upon acute*  
243 *MG-stress.*

244 To understand the role of stress-inducible HspA1A/HspA1B for processing of MG-modified  
245 proteins and MG-H1 accumulation, we generated HSPA1A/HSPA1B knockout MCECs using  
246 Crispr-Cas9 technology as shown in Fig S1. After 24 hrs of incubation with 500  $\mu$ M MG,  
247 HSPA1A/HSPA1B KO cells had higher MG-H1 levels as compared to WT cells (Fig 1A, Fig 1B).  
248 To analyze the capacity of both cell lines to clear MG-H1, medium was changed after 24 hrs  
249 and MG-H1 concentrations were measured after 24, 48 and 72 hrs. Compared to WT cells,  
250 HSPA1A/HSPA1B KO cells initially accumulated higher MG-H1 levels (Fig 1C). However, after  
251 changing the medium at 24 hrs to MG-free DMEM, both WT and HSPA1A/HSPA1B KO cells  
252 were able to clear MG-H1 adducts to a similar degree, reaching levels close to untreated  
253 controls after 48 hrs (Fig 1C).

254

255 *3.2 MG-stress induces mitochondrial heat shock proteins which is counteracted by*  
256 *HspA1A/HspA1B.*

257 As the PQC and HSP system is tightly regulated, the effective MG-H1 clearance in  
258 HSPA1A/HSPA1B KO cells could be achieved by compensatory upregulation of other HSPs.  
259 Therefore, we looked at levels of mRNA encoding different HSP subgroups that might be  
260 upregulated to compensate the loss of HSPA1A/HSPA1B. We found a decrease in HspA8 and  
261 HspB1 mRNA levels upon acute MG-stress in HSPA1A/HSPA1B KO cells (Fig S2A,B). In WT  
262 cells, mRNA encoding HspB1 and HspA5 was downregulated after short-term MG exposure  
263 (Fig S2B). Hsp90AA1 was slightly increased after MG-stress in both, WT and HSPA1A/HSPA1B  
264 KO cells. Dnajb1 (DnaJ homolog subfamily B member 1) mRNA was only upregulated

265 HSPA1A/HSPA1B KO cells and HspH1 only in WT cells after acute MG exposure (Fig S2A,B).  
266 mRNAs encoding the mitochondrial chaperones HspA9 and HspD1 were both induced upon  
267 acute MG-stress in WT as well as in HSPA1A/HSPA1B KO cells (Fig S2C). The co-chaperone of  
268 HspD1, Hsp10, showed no changes in mRNA expression upon MG-stress (Fig S2C). mRNA  
269 encoding Hsf1 (heat shock factor 1) dropped in HSPA1A/HSPA1B KO cells after short-term  
270 MG exposure (Fig S2D).

271 As mRNA levels encoding HspA9 and HspD1 were induced upon acute MG-stress, we also  
272 analyzed HspA9 and HspD1 protein expression after short-term MG exposure. In WT and  
273 HSPA1A/HSPA1B KO cells, HspA9 and HspD1 were exclusively expressed in the mitochondria  
274 and upregulated upon MG-stress (Fig 2A). However, induction of HspA9 (Fig 2B) and HspD1  
275 (Fig 2C) was higher in HSPA1A/HSPA1B KO cells.

276

### 277 *3.3 MG-stress induces mitochondrial biogenesis which is counteracted by HspA1a/HspA1B.*

278 The immunofluorescence (IF) stainings of MG-stressed cells suggested changes of  
279 mitochondrial network upon MG-stress. Therefore, we complemented IF imaging for Cox1  
280 (cytochrome c oxidase subunit 1) followed by a fully computed mitochondrial network  
281 analysis. Total Cox1 signal increased after acute MG-stress and was even stronger in  
282 HSPA1A/HSPA1B KO as compared to WT cells (Fig 2D). The same applied for mitochondrial  
283 count, mitochondrial branching, and mitochondrial total area (Fig 2E).

284

### 285 *3.4 Acute MG exposure reduces mitophagy and induces the mitochondrial unfolded protein* 286 *response.*

287 We next questioned the underlying mechanisms leading to induction of HspA9, HspD1 and  
288 mitochondrial mass upon MG-stress. Therefore, we looked at key-regulators of

289 mitochondrial fusion, fission, mitophagy and the mitochondrial unfolded protein response  
290 (mtUPR). mRNA encoding fusion proteins Mfn2 (Mitofusin-2) and Opa1 (Dynamin-like 120  
291 kDa protein, mitochondrial) were unchanged, whereas mRNA encoding Mfn1 (Mitofusin-1)  
292 was downregulated in WT and upregulated in HSPA1A/HSPA1B KO cells upon acute MG-  
293 stress (Fig 3A). The fission protein Drp1 (Dynamin-1-like protein) was induced in both cell  
294 lines, whereas Fis1 (mitochondrial fission 1 protein) was reduced in both cell lines on mRNA  
295 level after short-term MG exposure (Fig 3B). Proteins involved in mitophagy, namely Parkin,  
296 Pink1 (PTEN-induced kinase 1) and Bnip3 (BCL2/adenovirus E1B 19 kDa protein-interacting  
297 protein 3), were decreased on mRNA level upon MG-stress (Fig 3C). Components of the  
298 TIM23 complex, Timm17a (Mitochondrial import inner membrane translocase subunit  
299 Tim17-A) and Timm23 (Mitochondrial import inner membrane translocase subunit Tim23),  
300 were increased in HSPA1A/HSPA1B KO cells as markers of mitochondrial biogenesis or  
301 mtUPR (Fig 3D). Mitokines are known to be changed in mitochondrial stress conditions,  
302 therefore we also looked at mRNA levels encoding Fgf21 (Fibroblast growth factor 21) and  
303 Gdf15 (Growth/differentiation factor 15). We found that Fgf21 mRNA levels were decreased  
304 in both cell lines upon MG-stress, whereas Gdf15 was strongly induced in HSPA1A/HSPA1B  
305 KO cells (Fig 3E).

306

307 *3.5 Transcription factors involved in mitochondrial biogenesis are predominantly changed in*  
308 *HSPA1A/A1B KO cells upon MG-stress.*

309 To identify the transcription factors involved in induction of mitochondrial biogenesis, we  
310 looked at mRNA levels of Ppargc1a and Ppargc1b (Peroxisome proliferator-activated  
311 receptor gamma coactivator 1-beta), as they are known to be co-regulators of Nrf1 (Nuclear  
312 factor erythroid 2-related factor 1) and Nrf2 (Nuclear factor erythroid 2-related factor 2),

313 which promote the expression of Tfam (mitochondrial transcription factor A) (26, 46, 47).  
314 We found that Ppargc1a and Ppargc1b are downregulated upon MG-stress in WT cells (Fig  
315 4A). In HSPA1A/HSPA1B KO cells only Ppargc1a mRNA was downregulated (Fig 4A). Nrf2  
316 mRNA levels were unchanged, whereas Nrf1 expression increased in HSPA1A/HSPA1B KO  
317 cells but not in WT cells after acute MG exposure (Fig 4B). For transcription of mtDNA, the  
318 transcription factors Tfam and Tfb2m (mitochondrial transcription factor B2) are needed  
319 (48). Both were significantly upregulated in HSPA1A/HSPA1B KO but not in WT cells upon  
320 acute MG-stress (Fig 4C).

321 **4. Discussion**

322 We found that acute MG-Stress induces the expression of mitochondrial HspA9 and HspD1  
323 as well as mitochondrial biogenesis, both of which are counterregulated by stress-inducible  
324 HspA1A/HspA1B. These data suggest a prominent role of tight regulation of mitochondrial  
325 biogenesis by HSPs during acute MG-stress.

326

327 Increased MG-accumulation in endothelial cells has been linked to induction of the unfolded  
328 protein response (49). To show that mitochondrial homeostasis is of importance for securing  
329 ATP-dependent processes of the PQC, we knocked out HSPA1A/HSPA1B in mouse cardiac  
330 endothelial cells to increase proteotoxic and mitochondrial stress under acute MG exposure.  
331 Our hypothesis was, that loss of HSPA1A/HSPA1B would lead to increased MG-H1  
332 accumulation, toxicity, and mitochondrial dysfunction upon MG-stress.

333

334 We found that HSPA1A/HSPA1B KO cells accumulate higher MG-H1 levels as compared to  
335 WT cells, however MG-H1 clearance was highly efficient in the KO cells after the medium  
336 was changed. Indeed, MG-H1 concentrations in HSPA1A/HSPA1B KO cells dropped to the  
337 same level as in WT cells after further 24 hrs (Fig 1C). This might explain why we did not  
338 observe a significant increase in MG-toxicity in the HSPA1A/HSPA1B KO cells as compared to  
339 WT cells (data not shown). To identify compensatory mechanisms that would enable the  
340 HSPA1A/HSPA1B KO cells to clear MG-H1, we analyzed the expression levels of other HSPs.

341

342 Here we found the mitochondrial heat shock proteins HspA9 and HspD1 to be the strongest  
343 induced HSPs upon acute MG-stress, both on mRNA and protein levels (Fig 2A, B, C, Fig S2C).

344 Upregulation of HspA9 and HspD1 was present in WT and HSPA1A/HSPA1B KO cells,



345 however induction on protein level was pronounced in HSPA1A/HSPA1B KO cells upon MG-  
346 stress (Fig 2B, C). We first interpreted the induction of HspA9 and HspD1 expression as  
347 activation of the mtUPR due to rising proteotoxic stress. Therefore, we hypothesized that  
348 acute MG-stress would lead to disruption of mitochondrial homeostasis, which would be  
349 pronounced in the absence of HSPA1A/HSPA1B.

350

351 However, we found an increase in total mitochondria count, mitochondrial area, and  
352 mitochondrial branching (Fig 2E) after acute MG exposure. These changes were again even  
353 stronger in HSPA1A/HSPA1B KO cells and accompanied by downregulation of mRNA  
354 encoding proteins involved in fission and mitophagy (Fig 3B, C). Overall, these changes  
355 suggested that cells initiate mitochondrial biogenesis upon MG-stress, which was generally  
356 pronounced in the absence of HSPA1A/HSPA1B. The induction of mitochondrial biogenesis  
357 was further supported by the upregulation of transcription factors Nrf1, Tfam and Tfb2m in  
358 HSPA1A/HSPA1B KO cells, which are known mediators of mitochondrial biogenesis. We  
359 explained the increasing mitochondrial mass as a compensatory cellular mechanism to  
360 supply sufficient ATP levels for effective clearance of modified proteins under acute MG-  
361 stress. Hence, HSPA1A/HSPA1B KO cells would need stronger induction of mitochondrial  
362 biogenesis as they initially accumulate higher MG-H1 concentrations and have a higher  
363 demand in preventing aggregation of misfolded and damaged proteins. Therefore, the  
364 hormetic autofeedback induced by MG results in acute stimulation of mitochondrial  
365 biogenesis which is counterregulated by HspA1A/HspA1B thereby preventing from  
366 mitochondrial overstimulation and exhaustion.

367

368 If upregulation of mitochondrial mass would be a central defense mechanism to handle  
369 rising proteotoxic stress, induction of HspA9 could also be explained by increased  
370 translocation of proteins into the mitochondrial matrix during mitochondrial biogenesis, as it  
371 is the central subunit of the PAM (presequence translocase-associated motor) (50). Also,  
372 HspA9 could mirror the need for increased oxidative stress defense, as it has been described  
373 to play a key role in tumor survival especially under oxidative stress (51). HspA9 has been  
374 shown to mediate hypoxia induced preconditioning by preserving the activity of Cox1 and  
375 hence decreasing mitochondrial reactive oxygen species (ROS) production (52).  
376 Furthermore, downregulation of HspA9 resulted in increased autophagy and decreased  
377 pexophagy (53), which might explain why we observed a decrease in mitophagy upon  
378 upregulation of HspA9 via MG-stress.

379

380 HspD1 together with Hsp10 assists folding of proteins in the mitochondrial matrix including  
381 proteins involved in the synthesis of mitochondrial proteins, the respiratory chain and the  
382 mitochondrial PQC (54). Induction of HspD1 upon MG-stress could therefore indicate  
383 increased mitochondrial biogenesis as well as activation of the mtUPR. Interestingly,  
384 heterozygous HspD1 KO mice have been described to exhibit an altered adipose tissue  
385 metabolism with mitochondrial dysfunction and altered autophagy as well as local insulin  
386 resistance (55). HspD1 could therefore play a central role in maintaining mitochondrial  
387 function under increased metabolic stress conditions.

388

389 As mitochondrial dysfunction as well as mtUPR have been linked to Fgf21 and Gdf15, we  
390 looked at changes on mRNA levels after acute MG exposure. Both have been shown to be  
391 elevated in patients with metabolic syndrome and to be attenuated by exercise intervention

392 (56). However, data on Fgf21 and Gdf15 action are still inconclusive as they seem to prolong  
393 lifespan in model organisms (57, 58). Here, we found that Fgf21 was downregulated in WT  
394 and HSPA1A/HSPA1B KO cells upon acute MG-stress, whereas Gdf15 was dramatically  
395 induced in HSPA1A/HSPA1B KO cells. Therefore, both mitokines might signal mitochondrial  
396 changes under increased metabolic stress to other tissues possibly mediating adaptive  
397 mechanisms.

398

399 Taken together we found that acute MG-stress, as observed during increased metabolic flux,  
400 leads to induction of compensatory mechanisms, which consist of upregulation of the  
401 mitochondrial chaperones HspA9 and HspD1 as well as induction of mitochondrial  
402 biogenesis. These defense mechanisms were even pronounced in the absence of  
403 HSPA1A/HSPA1B, possibly because HSPA1A/HSPA1B KO cells initially accumulate higher MG-  
404 H1 levels upon MG-stress. To provide effective PQC and functioning of the ATP-dependent  
405 HspAs, cells must secure oxidative capacity which is maintained through mitochondrial  
406 biogenesis. However, mitochondrial dynamics need tight regulation as overstimulation of  
407 mitochondrial biogenesis would also increase oxidative stress and disturb mitochondrial  
408 homeostasis. Therefore, permanent induction of these compensatory mechanisms might  
409 lead to exhaustion and dysbalance of mitochondrial homeostasis as it is observed in diabetic  
410 complications. We found that stress-inducible HspA1A/HspA1B counteract this  
411 overstimulation of the MG-induced hormetic autofeedback during increased metabolic-  
412 stress.

413

414 **5. Conclusion**

415 Acute MG-stress induces mitochondrial HSPs as well as mitochondrial biogenesis in  
416 endothelial cells supporting the hypothesis of MG-induced hormesis. Tight regulation by  
417 HspA1A/HspA1B counteracts overstimulation of mitochondrial HspA9 and HspD1 as well as  
418 mitochondrial biogenesis. Therefore, HspA1A/HspA1B play a central role in maintaining the  
419 positive effects achieved by the MG-induced hormetic autofeedback and in prevention of  
420 mitochondrial exhaustion. Understanding of the HSP-regulated hormesis effects on  
421 mitochondrial content might reveal novel targets for the prevention and treatment of  
422 diabetic complications.

423 **Funding**

424 This work was supported by funding by the Deutsche Forschungsgemeinschaft (SFB 1118).

425

426 **Author contributions**

427 Conceptualization: J.Z., S.H.; Methodology: R.B., T.F., R.M., M.F.; Investigation: R.B., T.F.,

428 C.R.; Writing original Draft: J.Z., R.B.; Writing Review & Editing: T.F., M.M., S.H., J.S.;

429 Funding Acquisition: J.Z.; Supervision: J.Z.

430

431 **Declaration of interests**

432 None.

433

434 **Declaration of competing interest**

435 The authors declare no conflict of interest.

436

437 **Acknowledgments**

438 We thank Prof. Holger Lorenz, head of the imaging facility of the ZMBH, who programmed

439 the mitochondrial network plugins.

440 Furthermore, we want to thank Prof. Peter Nawroth for critical reading and discussion of the

441 manuscript.

442

443 **Supporting information**

444

## 445 References

- 446 1. Agathokleous E, Calabrese EJ. Hormesis: The dose response for the 21st century: The future  
447 has arrived. *Toxicology*. 2019;425:152249.
- 448 2. Ristow M, Zarse K, Oberbach A, Kloting N, Birringer M, Kiehntopf M, et al. Antioxidants  
449 prevent health-promoting effects of physical exercise in humans. *Proc Natl Acad Sci U S A*.  
450 2009;106(21):8665-70.
- 451 3. Koliaki C, Szendroedi J, Kaul K, Jelenik T, Nowotny P, Jankowiak F, et al. Adaptation of hepatic  
452 mitochondrial function in humans with non-alcoholic fatty liver is lost in steatohepatitis. *Cell*  
453 *Metab*. 2015;21(5):739-46.
- 454 4. Zemva J, Fink CA, Fleming TH, Schmidt L, Loft A, Herzig S, et al. Hormesis enables cells to  
455 handle accumulating toxic metabolites during increased energy flux. *Redox Biol*.  
456 2017;13:674-86.
- 457 5. Ravichandran M, Priebe S, Grigolon G, Rozanov L, Groth M, Laube B, et al. Impairing L-  
458 Threonine Catabolism Promotes Healthspan through Methylglyoxal-Mediated  
459 Proteohormesis. *Cell Metab*. 2018;27(4):914-25 e5.
- 460 6. Rabbani N, Ashour A, Thornalley PJ. Mass spectrometric determination of early and advanced  
461 glycation in biology. *Glycoconj J*. 2016;33(4):553-68.
- 462 7. Rabbani N, Thornalley PJ. Methylglyoxal, glyoxalase 1 and the dicarbonyl proteome. *Amino*  
463 *Acids*. 2012;42(4):1133-42.
- 464 8. Rabbani N, Thornalley PJ. Dicarbonyl proteome and genome damage in metabolic and  
465 vascular disease. *Biochem Soc Trans*. 2014;42(2):425-32.
- 466 9. Jensen TM, Vistisen D, Fleming T, Nawroth PP, Rossing P, Jorgensen ME, et al. Methylglyoxal  
467 is associated with changes in kidney function among individuals with screen-detected Type 2  
468 diabetes mellitus. *Diabet Med*. 2016;33(12):1625-31.
- 469 10. Lu J, Randell E, Han Y, Adeli K, Krahn J, Meng QH. Increased plasma methylglyoxal level,  
470 inflammation, and vascular endothelial dysfunction in diabetic nephropathy. *Clin Biochem*.  
471 2011;44(4):307-11.
- 472 11. Beisswenger PJ, Howell SK, Russell GB, Miller ME, Rich SS, Mauer M. Early progression of  
473 diabetic nephropathy correlates with methylglyoxal-derived advanced glycation end  
474 products. *Diabetes Care*. 2013;36(10):3234-9.
- 475 12. Saulnier PJ, Wheelock KM, Howell S, Weil EJ, Tanamas SK, Knowler WC, et al. Advanced  
476 Glycation End Products Predict Loss of Renal Function and Correlate With Lesions of Diabetic  
477 Kidney Disease in American Indians With Type 2 Diabetes. *Diabetes*. 2016;65(12):3744-53.
- 478 13. Hanssen NM, Stehouwer CD, Schalkwijk CG. Methylglyoxal and glyoxalase I in atherosclerosis.  
479 *Biochem Soc Trans*. 2014;42(2):443-9.
- 480 14. Roesen P, Ferber P, Tschoepe D. Macrovascular disease in diabetes: current status. *Exp Clin*  
481 *Endocrinol Diabetes*. 2001;109 Suppl 2:S474-86.
- 482 15. Tsilingiris D, Tzeravini E, Koliaki C, Dalamaga M, Kokkinos A. The Role of Mitochondrial  
483 Adaptation and Metabolic Flexibility in the Pathophysiology of Obesity and Insulin Resistance:  
484 an Updated Overview. *Curr Obes Rep*. 2021;10(3):191-213.
- 485 16. Rosca MG, Monnier VM, Szwedla LI, Weiss MF. Alterations in renal mitochondrial respiration  
486 in response to the reactive oxoaldehyde methylglyoxal. *Am J Physiol Renal Physiol*.  
487 2002;283(1):F52-9.
- 488 17. Rosca MG, Mustata TG, Kinter MT, Ozdemir AM, Kern TS, Szwedla LI, et al. Glycation of  
489 mitochondrial proteins from diabetic rat kidney is associated with excess superoxide  
490 formation. *Am J Physiol Renal Physiol*. 2005;289(2):F420-30.
- 491 18. Rabbani N, Thornalley PJ. Dicarbonyls linked to damage in the powerhouse: glycation of  
492 mitochondrial proteins and oxidative stress. *Biochem Soc Trans*. 2008;36(Pt 5):1045-50.
- 493 19. Song BJ, Akbar M, Abdelmegeed MA, Byun K, Lee B, Yoon SK, et al. Mitochondrial dysfunction  
494 and tissue injury by alcohol, high fat, nonalcoholic substances and pathological conditions  
495 through post-translational protein modifications. *Redox Biol*. 2014;3:109-23.

- 496 20. Rosenzweig R, Nillegoda NB, Mayer MP, Bukau B. The Hsp70 chaperone network. *Nat Rev*  
497 *Mol Cell Biol.* 2019;20(11):665-80.
- 498 21. Niforou K, Cheimonidou C, Trougakos IP. Molecular chaperones and proteostasis regulation  
499 during redox imbalance. *Redox Biol.* 2014;2:323-32.
- 500 22. Harding JJ, Beswick HT, Ajiboye R, Huby R, Blakytyn R, Rixon KC. Non-enzymic post-  
501 translational modification of proteins in aging. A review. *Mech Ageing Dev.* 1989;50(1):7-16.
- 502 23. Kampinga HH, Hageman J, Vos MJ, Kubota H, Tanguay RM, Bruford EA, et al. Guidelines for  
503 the nomenclature of the human heat shock proteins. *Cell Stress Chaperones.* 2009;14(1):105-  
504 11.
- 505 24. Havalova H, Ondrovicova G, Keresztesova B, Bauer JA, Pevala V, Kutejova E, et al.  
506 Mitochondrial HSP70 Chaperone System-The Influence of Post-Translational Modifications  
507 and Involvement in Human Diseases. *Int J Mol Sci.* 2021;22(15).
- 508 25. Shpilka T, Haynes CM. The mitochondrial UPR: mechanisms, physiological functions and  
509 implications in ageing. *Nat Rev Mol Cell Biol.* 2018;19(2):109-20.
- 510 26. Jornayvaz FR, Shulman GI. Regulation of mitochondrial biogenesis. *Essays Biochem.*  
511 2010;47:69-84.
- 512 27. Daugaard M, Rohde M, Jaattela M. The heat shock protein 70 family: Highly homologous  
513 proteins with overlapping and distinct functions. *FEBS Lett.* 2007;581(19):3702-10.
- 514 28. Dragovic Z, Broadley SA, Shomura Y, Bracher A, Hartl FU. Molecular chaperones of the  
515 Hsp110 family act as nucleotide exchange factors of Hsp70s. *EMBO J.* 2006;25(11):2519-28.
- 516 29. Gragerov A, Zeng L, Zhao X, Burkholder W, Gottesman ME. Specificity of DnaK-peptide  
517 binding. *J Mol Biol.* 1994;235(3):848-54.
- 518 30. van der Blik AM, Shen Q, Kawajiri S. Mechanisms of mitochondrial fission and fusion. *Cold*  
519 *Spring Harb Perspect Biol.* 2013;5(6).
- 520 31. Dai W, Lu H, Chen Y, Yang D, Sun L, He L. The Loss of Mitochondrial Quality Control in  
521 Diabetic Kidney Disease. *Front Cell Dev Biol.* 2021;9:706832.
- 522 32. Forbes JM, Thorburn DR. Mitochondrial dysfunction in diabetic kidney disease. *Nat Rev*  
523 *Nephrol.* 2018;14(5):291-312.
- 524 33. Patti ME, Butte AJ, Crunkhorn S, Cusi K, Berria R, Kashyap S, et al. Coordinated reduction of  
525 genes of oxidative metabolism in humans with insulin resistance and diabetes: Potential role  
526 of PGC1 and NRF1. *Proc Natl Acad Sci U S A.* 2003;100(14):8466-71.
- 527 34. Mootha VK, Lindgren CM, Eriksson KF, Subramanian A, Sihag S, Lehar J, et al. PGC-1alpha-  
528 responsive genes involved in oxidative phosphorylation are coordinately downregulated in  
529 human diabetes. *Nat Genet.* 2003;34(3):267-73.
- 530 35. Qu B, Jia Y, Liu Y, Wang H, Ren G, Wang H. The detection and role of heat shock protein 70 in  
531 various nondisease conditions and disease conditions: a literature review. *Cell Stress*  
532 *Chaperones.* 2015;20(6):885-92.
- 533 36. Hooper PL, Hooper PL. Inflammation, heat shock proteins, and type 2 diabetes. *Cell Stress*  
534 *Chaperones.* 2009;14(2):113-5.
- 535 37. Buraczynska M, Swatowski A, Buraczynska K, Dragan M, Ksiazek A. Heat-shock protein gene  
536 polymorphisms and the risk of nephropathy in patients with Type 2 diabetes. *Clin Sci (Lond).*  
537 2009;116(1):81-6.
- 538 38. Elshahed OM, Shaker OG. Heat Shock Protein 70 Gene Polymorphism in Egyptian Patients  
539 with Type 2 Diabetes Mellitus, with and without Nephropathy. *Saudi J Kidney Dis Transpl.*  
540 2020;31(4):787-95.
- 541 39. Moniruzzaman M, Ahmed I, Huq S, All Mahmud MS, Begum S, Mahzabin Amin US, et al.  
542 Association of polymorphism in heat shock protein 70 genes with type 2 diabetes in  
543 Bangladeshi population. *Mol Genet Genomic Med.* 2020;8(2):e1073.
- 544 40. Kurucz I, Morva A, Vaag A, Eriksson KF, Huang X, Groop L, et al. Decreased expression of heat  
545 shock protein 72 in skeletal muscle of patients with type 2 diabetes correlates with insulin  
546 resistance. *Diabetes.* 2002;51(4):1102-9.

- 547 41. Bruce CR, Carey AL, Hawley JA, Febbraio MA. Intramuscular heat shock protein 72 and heme  
548 oxygenase-1 mRNA are reduced in patients with type 2 diabetes: evidence that insulin  
549 resistance is associated with a disturbed antioxidant defense mechanism. *Diabetes*.  
550 2003;52(9):2338-45.
- 551 42. Atkin AS, Moin ASM, Al-Qaissi A, Sathyapalan T, Atkin SL, Butler AE. Plasma heat shock  
552 protein response to euglycemia in type 2 diabetes. *BMJ Open Diabetes Res Care*. 2021;9(1).
- 553 43. Bellini S, Barutta F, Mastrocola R, Imperatore L, Bruno G, Gruden G. Heat Shock Proteins in  
554 Vascular Diabetic Complications: Review and Future Perspective. *Int J Mol Sci*. 2017;18(12).
- 555 44. Sayed KM, Mahmoud AA. Heat shock protein-70 and hypoxia inducible factor-1alpha in type  
556 2 diabetes mellitus patients complicated with retinopathy. *Acta Ophthalmol*.  
557 2016;94(5):e361-6.
- 558 45. Gruden G, Bruno G, Chaturvedi N, Burt D, Pinach S, Schalkwijk C, et al. ANTI-HSP60 and ANTI-  
559 HSP70 antibody levels and micro/ macrovascular complications in type 1 diabetes: the  
560 EURODIAB Study. *J Intern Med*. 2009;266(6):527-36.
- 561 46. Virbasius JV, Scarpulla RC. Activation of the human mitochondrial transcription factor A gene  
562 by nuclear respiratory factors: a potential regulatory link between nuclear and mitochondrial  
563 gene expression in organelle biogenesis. *Proc Natl Acad Sci U S A*. 1994;91(4):1309-13.
- 564 47. Wu Z, Puigserver P, Andersson U, Zhang C, Adelmant G, Mootha V, et al. Mechanisms c  
565 ontrolling mitochondrial biogenesis and respiration through the thermogenic coactivator  
566 PGC-1. *Cell*. 1999;98(1):115-24.
- 567 48. Shokolenko IN, Alexeyev MF. Mitochondrial transcription in mammalian cells. *Front Biosci*  
568 (Landmark Ed). 2017;22:835-53.
- 569 49. Irshad Z, Xue M, Ashour A, Larkin JR, Thornalley PJ, Rabbani N. Activation of the unfolded  
570 protein response in high glucose treated endothelial cells is mediated by methylglyoxal. *Sci*  
571 *Rep*. 2019;9(1):7889.
- 572 50. Tang JX, Thompson K, Taylor RW, Olahova M. Mitochondrial OXPHOS Biogenesis: Co-  
573 Regulation of Protein Synthesis, Import, and Assembly Pathways. *Int J Mol Sci*. 2020;21(11).
- 574 51. Pagliarone AC, Castañeda ED, Santana JPP, de Oliveira CAB, Robeldo TA, Teixeira FR, et al.  
575 Mitochondrial heat shock protein mortalin as potential target for therapies based on  
576 oxidative stress. *Photodiagnosis Photodyn Ther*. 2021;34:102256.
- 577 52. Deng YZ, Xiao L, Zhao L, Qiu LJ, Ma ZX, Xu XW, et al. Molecular Mechanism Underlying  
578 Hypoxic Preconditioning-Promoted Mitochondrial Translocation of DJ-1 in  
579 Hypoxia/Reoxygenation H9c2 Cells. *Molecules*. 2019;25(1).
- 580 53. Jo DS, Park SJ, Kim AK, Park NY, Kim JB, Bae JE, et al. Loss of HSPA9 induces peroxisomal  
581 degradation by increasing pexophagy. *Autophagy*. 2020;16(11):1989-2003.
- 582 54. Bie AS, Cömert C, Körner R, Corydon TJ, Palmfeldt J, Hipp MS, et al. An inventory of  
583 interactors of the human HSP60/HSP10 chaperonin in the mitochondrial matrix space. *Cell*  
584 *Stress Chaperones*. 2020;25(3):407-16.
- 585 55. Hauffe R, Rath M, Schell M, Ritter K, Kappert K, Deubel S, et al. HSP60 reduction protects  
586 against diet-induced obesity by modulating energy metabolism in adipose tissue. *Mol Metab*.  
587 2021;53:101276.
- 588 56. Chang JS, Namkung J. Effects of Exercise Intervention on Mitochondrial Stress Biomarkers in  
589 Metabolic Syndrome Patients: A Randomized Controlled Trial. *Int J Environ Res Public Health*.  
590 2021;18(5).
- 591 57. Zhang Y, Xie Y, Berglund ED, Coate KC, He TT, Katafuchi T, et al. The starvation hormone,  
592 fibroblast growth factor-21, extends lifespan in mice. *Elife*. 2012;1:e00065.
- 593 58. Wang X, Chrysovergis K, Kosak J, Kissling G, Streicker M, Moser G, et al. hNAG-1 increases  
594 lifespan by regulating energy metabolism and insulin/IGF-1/mTOR signaling. *Aging (Albany*  
595 *NY)*. 2014;6(8):690-704.

596



1 **Fig 1.** MG-H1 accumulation is higher in HSPA1A/HSPA1B KO compared to WT cells upon  
2 acute MG-stress. Immunofluorescence staining with an anti-MG-H1 antibody of WT and  
3 HSPA1A/HSPA1B KO cells was performed after MG-treatment with 500  $\mu$ M for 24 hrs (A) and  
4 quantified in (B). (C) MG-H1 clearance was monitored after 24 hrs MG-treatment in  
5 HSPA1A/HSPA1B KO vs. WT cells. Results are shown as means  $\pm$  SD of at least 3 independent  
6 experiments. Two-way ANOVA with Šídák's multiple comparisons test was performed for  
7 statistical analysis, \* $p < 0.05$ , \*\* $p < 0.01$ , \*\*\* $p < 0.001$ .

8

9 **Fig 2.** MG-stress induces mitochondrial heat shock proteins and mitochondrial biogenesis.  
10 WT and HSPA1A/A1B KO cells were treated with MG for 24 hrs, probed for the mitochondrial  
11 HSPs HspA9 and HspD1, analyzed by IF imaging (A) and quantified (B, C). For analysis of  
12 changes in mitochondrial morphology upon MG-stress, WT and HSPA1A/A1B KO cells were  
13 probed with an anti-Cox1 antibody, imaged via IF, followed by a fully computed analysis of  
14 mitochondrial network parameters. (D) Quantification of Cox1 signal. (E) Quantification of  
15 mitochondrial count, branching and total area. Results are shown as means  $\pm$  SD of at least  
16 3 independent experiments. Two-way ANOVA with Šídák's multiple comparisons test was  
17 performed for statistical analysis, \* $p < 0.05$ , \*\* $p < 0.01$ , \*\*\* $p < 0.001$ .

18

19 **Fig 3.** Acute MG exposure reduces mitophagy and induces the mitochondrial unfolded  
20 protein response. WT and HSPA1A/A1B KO cells were treated for 12 hrs with 500  $\mu$ M MG  
21 before mRNA analysis. (A) Levels of mRNA encoding fusion proteins Mfn1, Mfn2, Opa1. (B)  
22 Levels of mRNA encoding fission proteins Drp1 and Fis1. (C) mRNA expression levels of  
23 mitophagy mediators Parkin, Pink1 and Bnip3. (D) mRNA expression of the key components  
24 of the TIM23 complex, Timm17a and Timm23. (E) Levels of mRNA encoding the mitokines

25 Fgf21 and Gdf15. Results are shown as means  $\pm$  SD of at least 3 independent experiments.

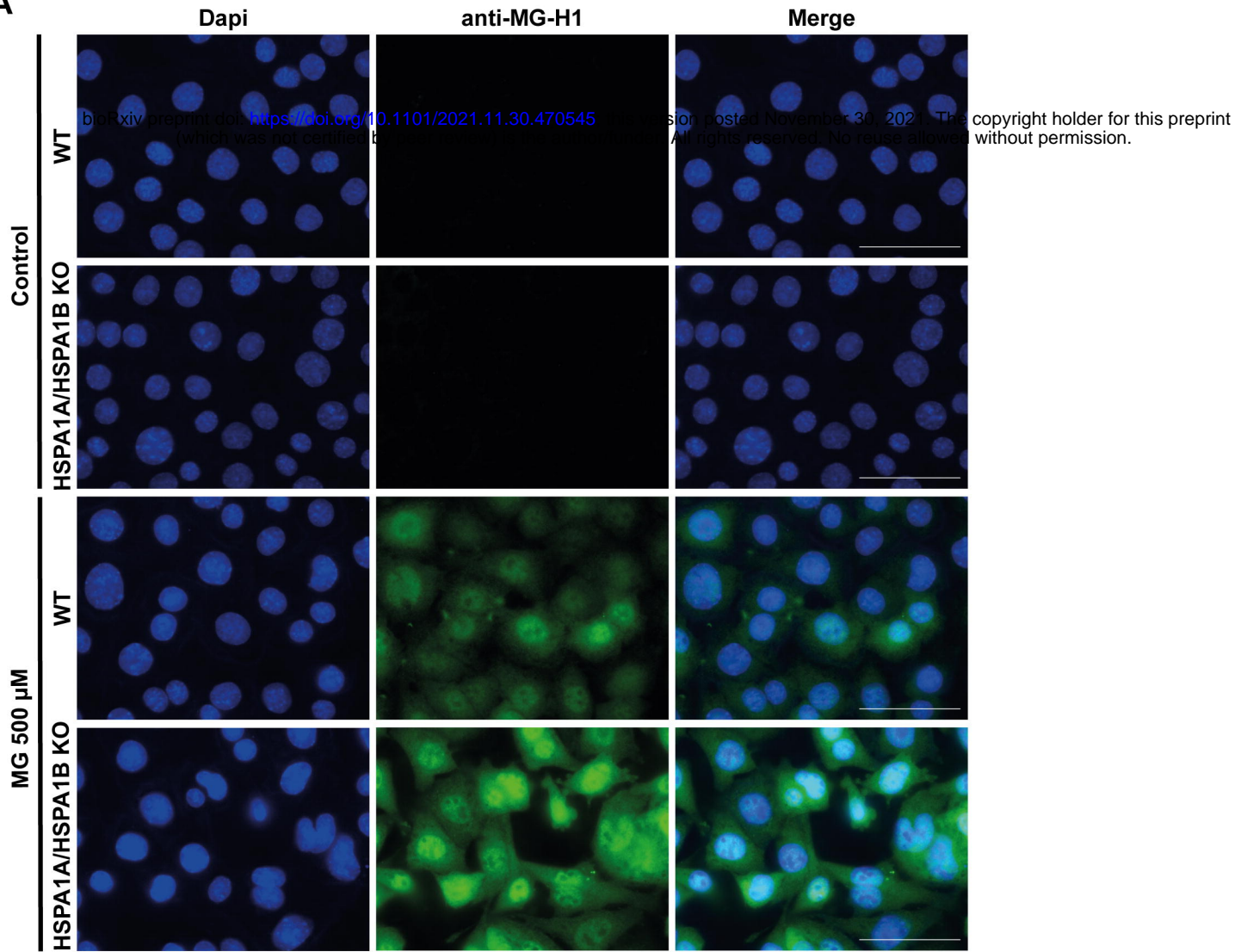
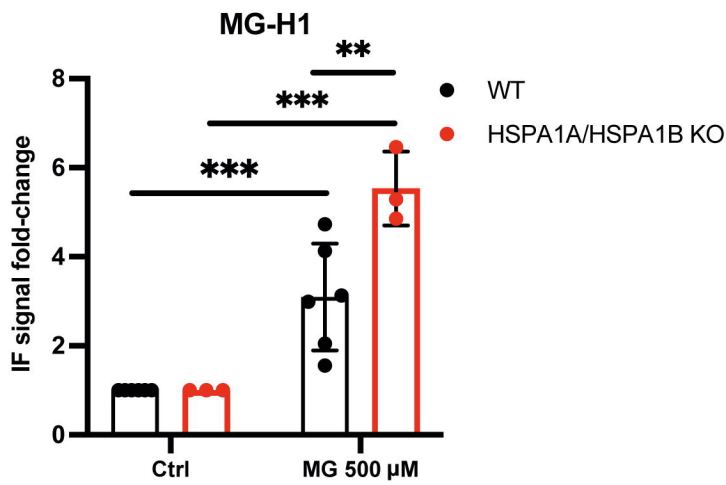
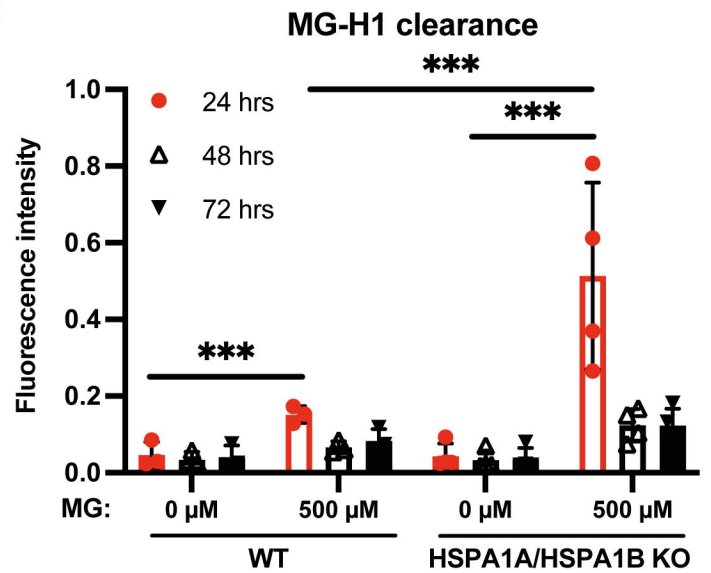
26 Two-way ANOVA with Šídák's multiple comparisons test was performed for statistical  
27 analysis, \*p<0.05, \*\*p<0.01, \*\*\*p<0.001.

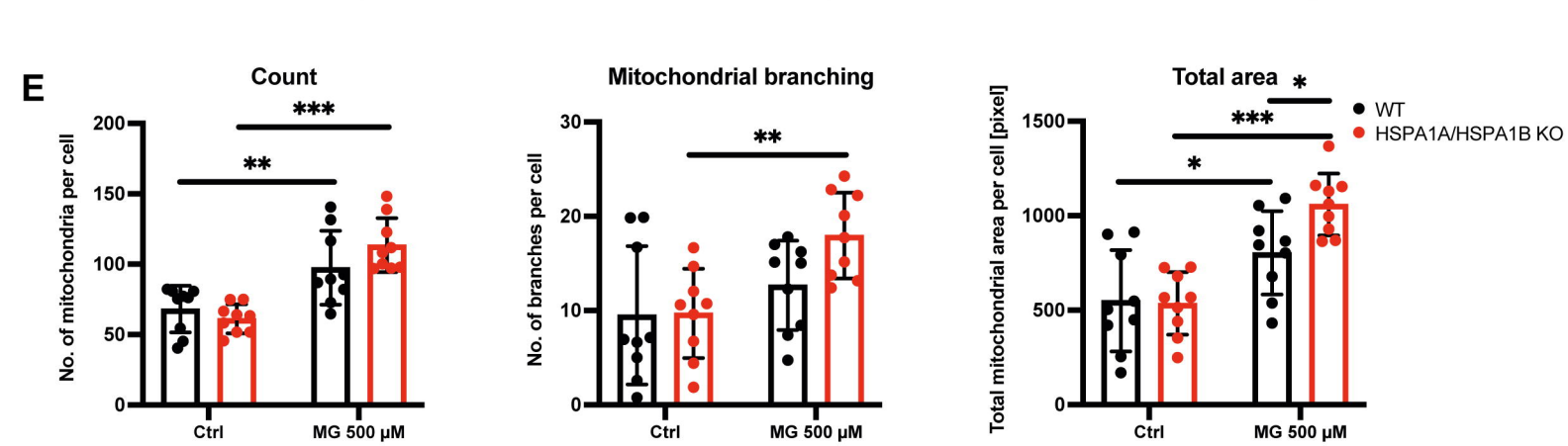
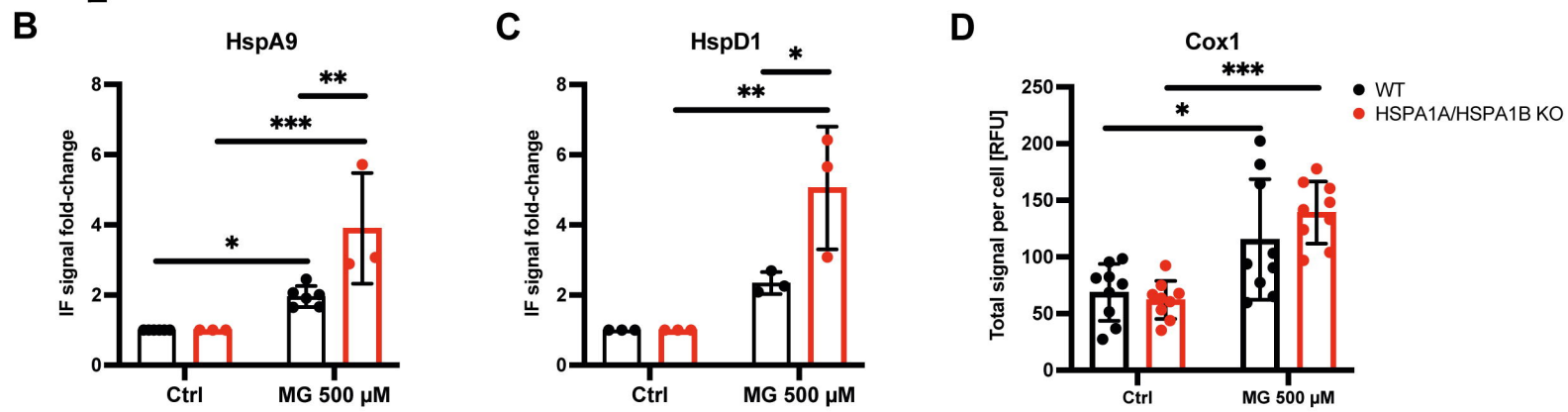
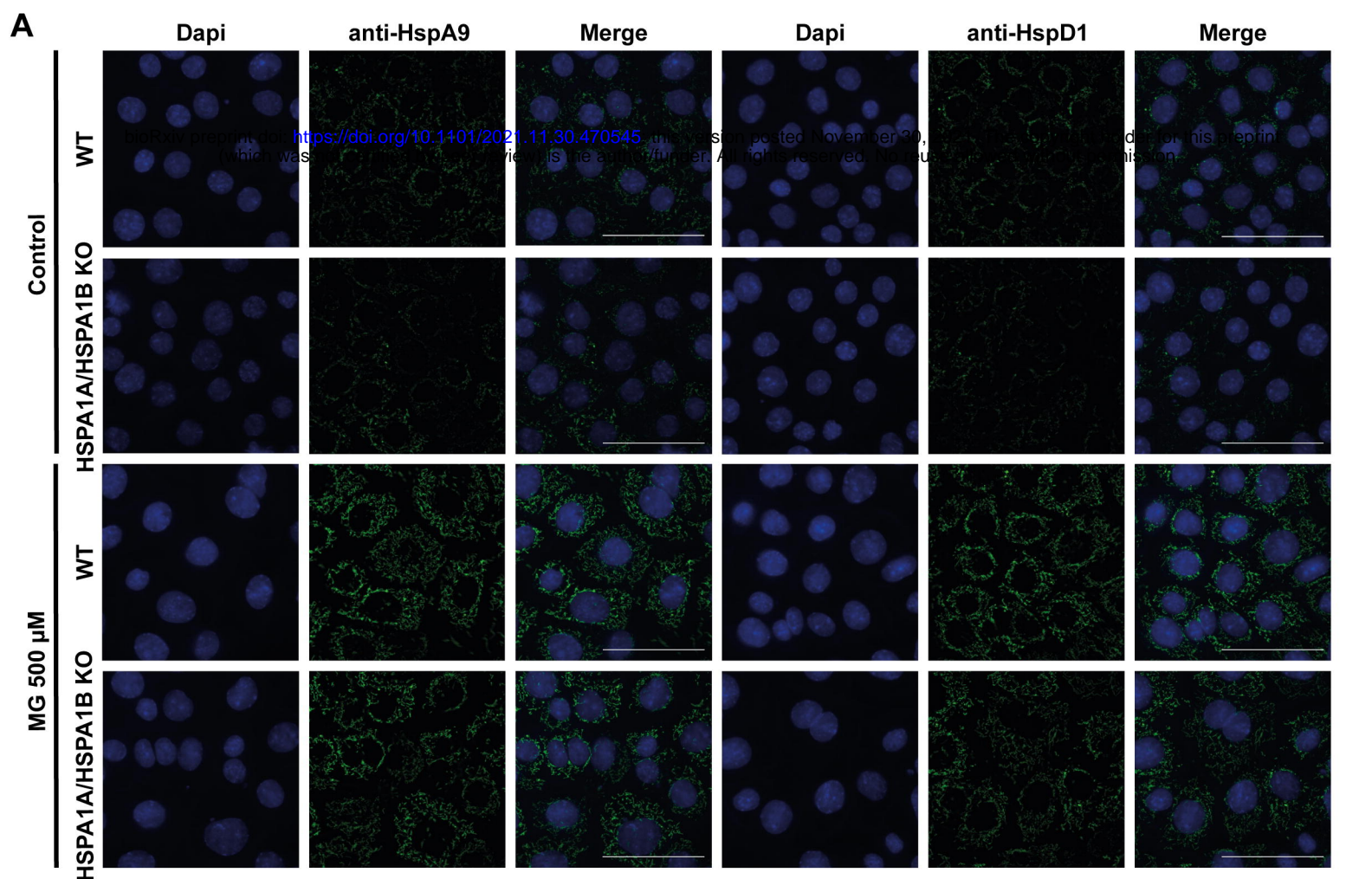
28

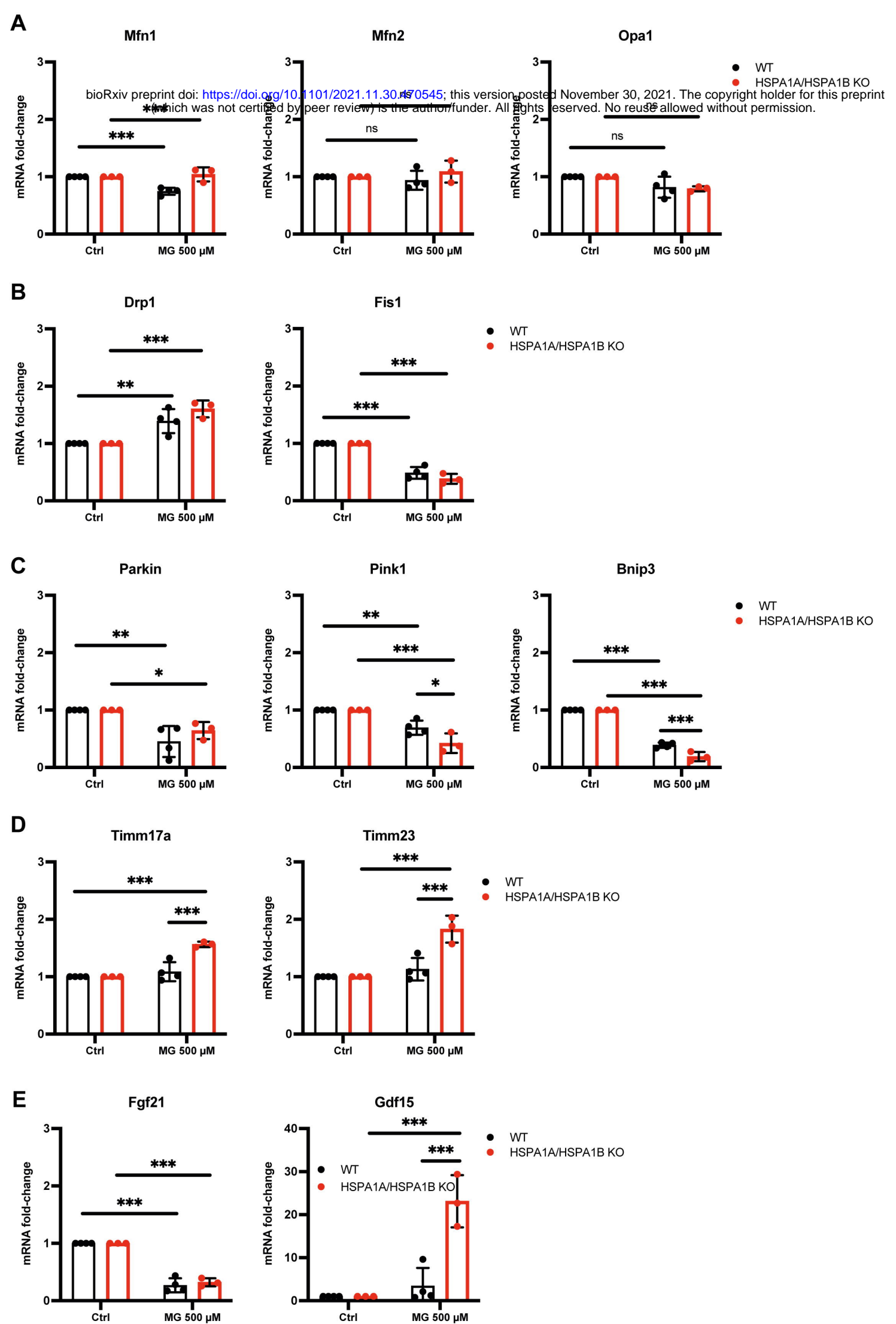
29 **Fig 4.** Transcription factors involved in mitochondrial biogenesis are predominantly changed  
30 in HSPA1A/A1B KO cells upon MG-stress. Levels of mRNA encoding transcription factors  
31 regulating mitochondrial biogenesis were analyzed in WT and HSPA1A/A1B KO cells after 12  
32 hrs incubation with 500  $\mu$ M MG. (A) mRNA expression of Ppargc1a and Ppargc1a, (B) of Nrf1  
33 and Nrf2, (C) of Tfam and Tfb2m. Results are shown as means  $\pm$  SD of at least 3 independent  
34 experiments. Two-way ANOVA with Šídák's multiple comparisons test was performed for  
35 statistical analysis, \*p<0.05, \*\*p<0.01, \*\*\*p<0.001.

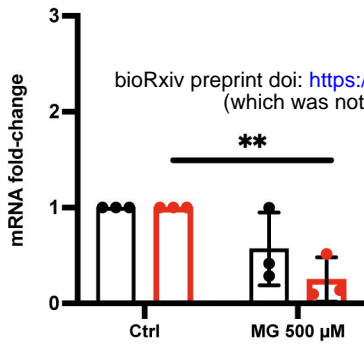
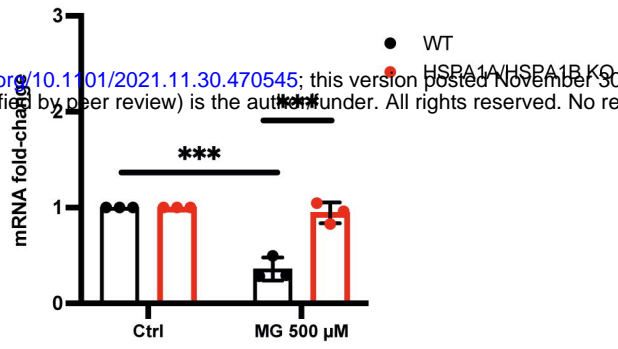
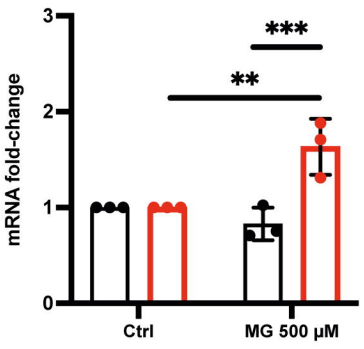
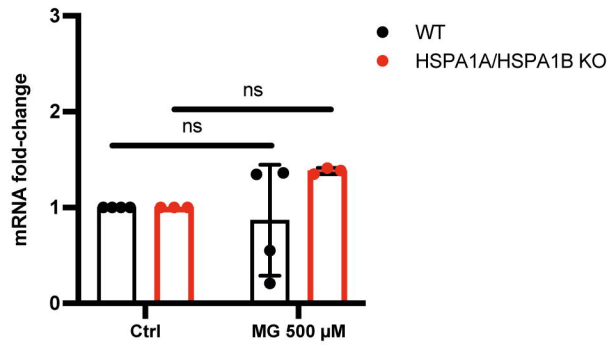
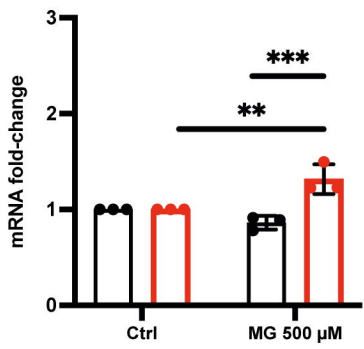
36

37

**A****B****C**





**A****Ppargc1a****Ppargc1b****B****Nrf1****Nrf2****C****Tfam****Tfb2m**